

## Close-packed atomic bromine up to 230 GPa

E. Edmund<sup>1,\*</sup>, M. H. Dalsaniya<sup>2,3</sup>, R. T. Howie<sup>1,4</sup>, E. Greenberg<sup>5,‡</sup>, V. B. Prakapenka<sup>5</sup>, M. Peña-Álvarez<sup>4</sup>,  
M. Hanfland<sup>6</sup>, P. Dalladay-Simpson<sup>1,§</sup>, D. Kurzydłowski<sup>3</sup>, and A. Hermann<sup>4,||</sup>

<sup>1</sup>*Centre for High Pressure Science and Technology Advanced Research (HPSTAR), Shanghai, China*


<sup>2</sup>*Faculty of Materials Science and Engineering, Warsaw University of Technology, Włocławska 141, 02-507 Warsaw, Poland*

<sup>3</sup>*Faculty of Mathematics and Natural Sciences, Cardinal Stefan Wyszyński University in Warsaw, 01-938 Warsaw, Poland*

<sup>4</sup>*Centre for Science at Extreme Conditions and School of Physics and Astronomy, University of Edinburgh, Edinburgh EH9 3FD, United Kingdom*

<sup>5</sup>*GeoSoilEnviroCARS, University of Chicago, Chicago, Illinois 60637, USA*

<sup>6</sup>*ESRF, 38000 Grenoble, France*

 (Received 4 February 2025; revised 6 August 2025; accepted 9 September 2025; published 14 October 2025)

In the present study, the phase transitions of bromine have been investigated using high-pressure x-ray diffraction experiments and *ab initio* calculations up to 230 and 180 GPa, respectively. At pressures beyond molecular dissociation, *Immm*, *I4/mmm*, and *Fm3̄m* phases are found, in agreement with the structural sequence found for iodine. We find that the phase transitions are remarkably sluggish—most notably for the *Immm*-*I4/mmm* transition where the two phases coexist from 105(7) to 163(10) GPa, and the transition is observed to result in a small volume discontinuity. By symmetry, these phases are directly related, and *ab initio* calculations show no energetic barrier between them. However, calculations of the static enthalpy landscape of the close-packed phases under pressure reveal a highly anharmonic potential energy surface, resulting in strong entropic effects when investigating the phase transitions of dissociated bromine.

DOI: [10.1103/rbsx-vqhf](https://doi.org/10.1103/rbsx-vqhf)

## I. INTRODUCTION

The halogens iodine, bromine, and chlorine have been studied by a variety of techniques, due to scientific interest in understanding the physics of molecular metallization via band overlap [1–5]. Iodine, bromine, and chlorine all exhibit the same structural motifs while evolving from a molecular insulator to a metallic solid [6–8]. Despite the typical scaling behavior of elements of the same period at high pressure (see, e.g., Refs. [9,10]), it is expected that the structures of the lighter halogens hydrogen and fluorine differ substantially from their heavier analogs [11,12]. As molecular chlorine is observed to metallize and dissociate above 200 and 265 GPa, respectively [8], iodine and bromine are likely the only halogens for which the full sequence of structural transitions from molecular solids to close-packed metals are observable at the pressures of conventional diamond anvil cell (DAC) techniques [13–15].

At low temperatures and ambient pressure, iodine, bromine, and chlorine solidify in the *Cmce* structure, composed of zigzag molecular chains along the *ab* plane, with large distances between successive planes of molecules [16,17]. Deviations from the ambient pressure *Cmce* structure

have been observed by x-ray diffraction for chlorine and iodine [8,18,19], and the splitting of Raman modes related to molecular libration has been observed for iodine, bromine, and chlorine [7,8,19]. Changes in interatomic distances determined by extended x-ray absorption fine structure (EXAFS) in iodine and bromine [20,21] have been proposed to indicate the presence of a structural transition from the *Cmce* phase into a different molecular structure at 25 and 8 GPa, respectively. Two further second-order phase transformations take place upon increasing pressure to form a face-centered-orthorhombic motif, which is incommensurately modulated along the direction of intramolecular bonding [19,22–24]. Metallization of the solid via band overlap is expected to occur prior to full molecular dissociation for chlorine, bromine, and iodine [8,14,25]. The structural complexity which coincides with the molecular dissociation of  $I_2$  and  $Br_2$  into metallic close-packed solids can be viewed as an attempt to minimize the strain between the molecular (*Cmce*) and dissociated (*Immm*) lattices [26]. Iodine, bromine, and chlorine are all observed to undergo a first-order phase transition into a body-centered-orthorhombic phase (*Immm*) which represents the first of a series of monatomic, metallic phases at successively higher pressures [2,8,14]. In iodine, a further second-order transformation to a body-centered-tetragonal (*I4/mmm*) and first-order transformation into a face-centered-cubic (fcc) (*Fm3̄m*) phase are observed [13,15,27]. The fcc phase in particular is expected to be the stable metallic phase of the period 3–5 halogens up to TPa pressures [15,28]. Bromine has not been studied above 110 GPa [7,14,24], and metallic phases beyond the *Immm* structure have yet to be observed. Recent work has found iodine to adopt a *Pm3̄n* structure, only

\*Present address: Universität-Münster, Corrensstrasse 24, 48149 Münster, Germany

†Contact author: eric.edmund@uni-muenster.de

‡Present address: SNRC, Applied Physics Department, Yavne 81800, Israel.

§Contact author: phillip.dalladay-simpson@hpstar.ac.cn

||Contact author: a.hermann@ed.ac.uk

predicted for dissociated fluorine [12], when quenched from a high temperature at pressures near the stability field of the  $Fm\bar{3}m$  structure at 48–51 GPa [29].

In order to better understand the dense solid halogens, structural investigations of close-packed bromine are presented through a combination of high-pressure experiments and first-principles calculations. Experiments employ the generation of static high pressures using diamond anvil cells up to 230 GPa, coupled with synchrotron x-ray diffraction. First-principles calculations use density-functional theory to investigate the ground state and potential energy surface (PES) of metallic bromine at pressures between 90 and 180 GPa. In doing so, we follow the evolution of bromine from a molecular solid to a cubic metal at extreme pressures.

## II. METHODS

### A. Experimental methods

Bromine is liquid at ambient pressure and temperature, and its high toxicity via inhalation and high partial pressure requires careful handling. High-purity bromine (Sigma Aldrich, >99.99% purity, Lot No. SHBJ1858) was loaded as a polycrystalline solid at cryogenic temperatures into the sample chambers of two diamond anvil cells. For run 1, double-bevelled 30- $\mu\text{m}$  culet diamonds were employed, with bevels of 100 and 300  $\mu\text{m}$  diameter. For run 2, single-bevelled 70- $\mu\text{m}$  culets were used with a bevel width of 300  $\mu\text{m}$ . For both runs, the diamonds were equipped with 250- $\mu\text{m}$ -thick Re gaskets which also served as the pressure marker for both experiments [30]. No additional pressure marker was added, due to the small sample chamber dimensions, potential reactivity with the sample, and the possibility to introduce additional contaminants.

Synchrotron powder x-ray diffraction measurements were carried out at beamlines GSECARS 13-IDD (Advanced Photon Source, USA) for run 1 and ID15b (European Synchrotron Radiation Facility, France) for run 2. Diffraction images were collected in transmission geometry using an Pilatus 3x 1M CdTe or the Eiger 2 CdTe 9M detectors on 13-IDD and ID15b, respectively. The two-dimensional (2D) images were azimuthally integrated to generate 1D diffraction patterns using the DIOPTAS software package [31]. At 13-IDD, the x-ray beam dimensions were approximately 3  $\mu\text{m} \times 2.5 \mu\text{m}$  (vertical by horizontal) at an x-ray wavelength of 0.3344 Å, and collection geometry was calibrated using an LaB<sub>6</sub> standard. For run 1, diffraction images were collected without varying the angle between the compression axis and x-ray beam, in order to minimize the Re signal of the collected diffraction image. At ID15b, x-ray beam dimensions were approximately 3  $\mu\text{m} \times 3 \mu\text{m}$  (horizontal by vertical) at an x-ray wavelength of 0.4105 Å, and the diffraction images were collected while varying the angle of the cell by  $\pm 2.5^\circ$  in order to sample a wider range of crystallite orientations. All diffraction data have been analyzed using the Le Bail method as implemented in JANA2006 [32]. Rietveld refinement is not used in the present study due to the effect of stress and texture imparted by nonhydrostatic compression of the bromine samples.

Reported pressures are determined from the unit cell volume of the Re gasket, and in run 1 pressures were also

measured employing the shift of the  $T_{2g}$  diamond phonon of the stressed diamond anvil [33]. Pressures measured using the Raman signal of the stressed diamond were typically 5–10 GPa higher than that measured by the unit cell volume of Re at Mbar pressures, which is comparable in magnitude to differences in pressure calibration between Akahama and Kawamura [33] and Anzellini *et al.* [30]. In run 1 the error in pressure for each diffraction measurement is 5% of total pressure and the difference in pressure between Raman and Re pressures, added in quadrature. For run 2, the larger sample sizes afforded nearly rhenium-free diffraction up to  $\sim 152$  GPa—consequently the pressure gradients between sample volume at the center of the cell and at the gasket position and possible changes in pressure between measurement positions have been estimated based on the available equation of state of  $Cmce$  bromine [6] for the molecular phases, or the fitted equation of state for  $Immm$  bromine established here. This error in pressure is combined further with a 5% uncertainty in total pressure. The use of the rhenium gasket as a pressure calibrant leads to a systematic uncertainty of up to 5 GPa for pressures below 150 GPa and up to 10 GPa at higher pressures [30], which is comparable to uncertainties reported here.

### B. Computational methods

Density-functional theory (DFT) calculations were performed in order to compute the potential energy surface (PES) of the  $Immm$ - $I4/mmm$ - $Fm\bar{3}m$  phase transition sequence, where we used the conventional cell of orthorhombic  $Immm$  which contains two bromine atoms in (0,0,0) and  $(\frac{1}{2}, \frac{1}{2}, \frac{1}{2})$  special positions. At each pressure point, we generated structures with different ratios of lattice vector lengths ( $1.00 < b/a < 1.10$ ;  $1.40 < c/a < 1.95$ ) and optimized their volume while keeping the shape of the cell unchanged. The  $I4/mmm$  structure corresponds to  $b/a = 1$ , and the  $Fm\bar{3}m$  phase to  $c/a = \sqrt{2} = 1.414$ . Calculations conducted for pressure ranges from 90 to 180 GPa, yielded enthalpies ( $H$ ) which were used for construction of the PES under the assumption that  $H(a, b, c) = H(b, a, c)$ , i.e., we assumed an equivalence of the PES with respect to an exchange in the  $a$  and  $b$  lattice vectors.

Geometry optimizations were performed using the hybrid Heyd-Scuseria-Ernzerhof (HSE06) functional [34] with van der Waals corrections (D3 method of Grimme), [35,36] in the Vienna *ab initio* simulation package (VASP 6.3.2) [37,38]. The calculations employed the projector augmented-wave (PAW) method, where the  $4s$  and  $4p$  states were treated explicitly. The kinetic-energy cutoff for the plane-wave basis set was set to 800 eV. The reciprocal space was sampled with a dense  $19 \times 19 \times 12$  Monkhorst-Pack  $k$ -point mesh [39]. The threshold value for the electronic minimization was set to  $10^{-8}$  eV, and the tolerance in the optimized pressure was below 1 kbar. The computational expense of very dense  $k$ -point sampling and the use of hybrid exchange-correlation functionals is necessary to accurately model the phase transition pressures and the PES of bromine [26,40]. Standard generalized gradient functionals, while qualitatively accounting for the effects reported here, systematically underestimate the transition pressures across all known bromine phases [41].

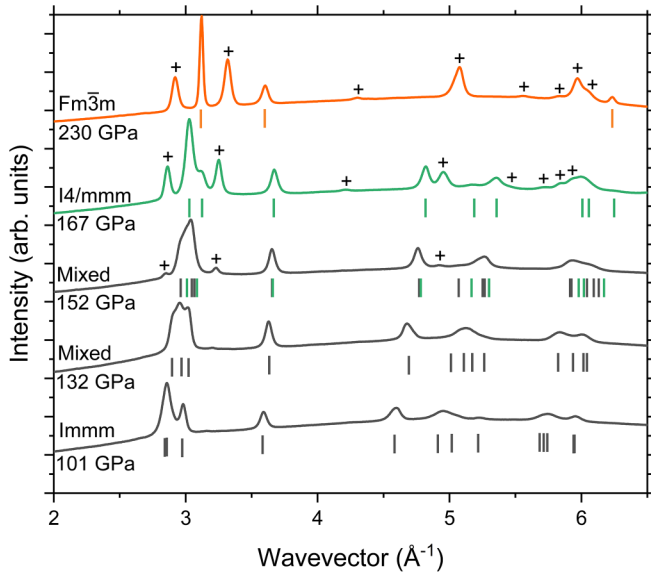


FIG. 1. X-ray diffraction patterns of the dissociated body-centered-orthorhombic ( $Immm$ , phase II), body-centered-tetragonal ( $I4/mmm$ , phase V), and face-centered-cubic ( $Fm\bar{3}m$ , phase VI) structures of dense bromine. Crosses indicate reflections originating from the rhenium gasket. Gray, green, and orange ticks correspond to refined peak positions for  $Immm$ ,  $I4/mmm$ , and  $Fm\bar{3}m$  reflections, respectively. Identification of mixed  $Immm$  and  $I4/mmm$  phases is described in more detail in the main text and Fig. S1 [42].

### III. RESULTS AND DISCUSSION

Figure 1 shows diffraction patterns of the observed high-pressure phases for close-packed bromine. The  $Immm$  structure (phase II) has been previously observed [14] up to 89 GPa, and results from the equalization of intermolecular and intramolecular spacings between successive bromine molecules due to bond dissociation. This orthorhombic structure is layered, with the  $a$ - $b$  plane corresponding to the former plane of intermolecular bonding in the lower-pressure molecular phases. The  $I4/mmm$  structure (phase V) discovered here is observed as a pure phase above 165 GPa, and results from the equalization of interatomic distances between bromine atoms lying on the  $a$ - $b$  plane; the  $Immm$  structure is equivalent to the  $I4/mmm$  structure when  $b/a = 1$ . The observed  $Fm\bar{3}m$  (phase VI) structure, which forms above 180 GPa, results from the equalization of intralayer ( $a$ - $b$  plane) and interlayer ( $c$ -axis) nearest-neighbor distances in the  $I4/mmm$  structure which forms an isotropic, face-centered structure. The  $Immm$  structure is equivalent to the  $Fm\bar{3}m$  structure when  $b/a = 1$  and  $c/a = \sqrt{2}$  [41]. In Figs. 1 and 2, transitions from the molecular phases to the close-packed  $Immm$  phase, as well as the  $I4/mmm$  to  $Fm\bar{3}m$  transitions are first order and their transition pressures are comparable to recent theoretical investigations of dense bromine [26], which is consistent with the change in coordination number which occurs during these transitions [6]. However, experimental observations of the  $Immm$  to  $I4/mmm$  transition appear to indicate a departure from previous investigations on iodine, as well as bromine theory [13,26].

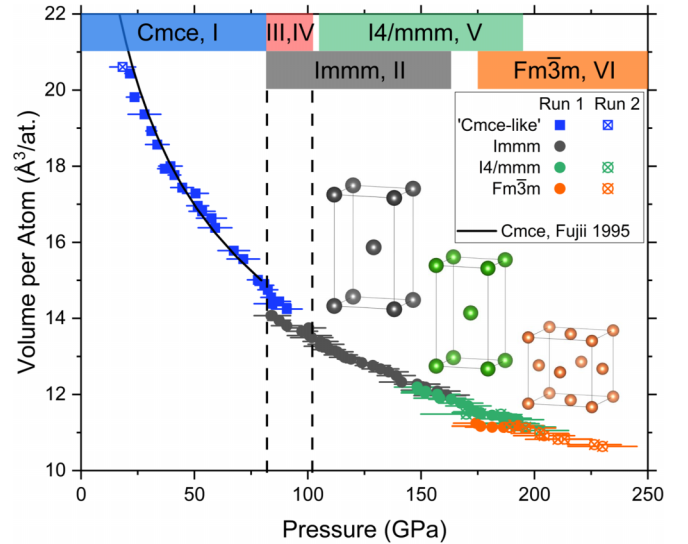


FIG. 2. Experimental pressure-volume relations of bromine. The solid black line indicates the equation of state of  $Cmce$  bromine [14]. Gray, green, and orange volumes and structures indicate the observed close-packed structures in the present study. Vertical dashed lines indicate the transition region between molecular and dissociated phases [7,24]. Colored boxes indicate the pressure range where each phase is observed in the present study. The successive transitions between  $Cmce$  phase I and incommensurate  $Fmm2$  phases III and IV are not resolvable under nonhydrostatic conditions [19,22,43], and their stability fields are taken from the literature [7,24].

Experimentally, the  $Immm$  and  $I4/mmm$  phases are observed to coexist as a mixed phase from 105 to 163 GPa, above which point only the  $I4/mmm$  phase is observed. This cannot be reconciled by the effect of pressure gradients as bromine is soft; measurements of bromine volume at the center of the DAC and near the Re gasket give volumes which differ by no more than 1–2 GPa at all pressures. The coexisting  $I4/mmm$  and  $Immm$  phases exhibit a small volume difference which relates to a small difference in the length of the  $c$  axis. Discontinuous changes in  $Immm$  reflection positions and intensities are observed over the pressure range of stability, which cannot be reproduced by a single phase (Fig. S1) [42]. In Figs. 1 and 2 the  $le$  Bail refinement of the two-phase mixture stabilized above 145 GPa.

A transition between the  $Immm$  and  $I4/mmm$  structures with a finite-volume change is in contrast to studies of iodine, where the transition is second order [13]. There are no symmetry constraints on the phase transitions between these phases, raising questions about the origins of this result. To gain insight into the transition sequence of dissociated bromine, we turn to advanced *ab initio* calculations to investigate the evolution of the static PES of bromine under pressure. In these calculations, the static enthalpy of close-packed bromine is investigated as a function of  $c/a$  and  $b/a$  ratio. Plots of relative enthalpy per atom as a function of  $c/a$  and  $b/a$  ratios are shown in Fig. 3. The potential energy surface of  $Immm$  bromine is found to be highly anharmonic and variations of lattice shape on the order of 5%–10% change the enthalpy of the structure by 5 meV/atom or less. 300 K corresponds to an energy scale of  $\sim 25$  meV/atom, leading to the



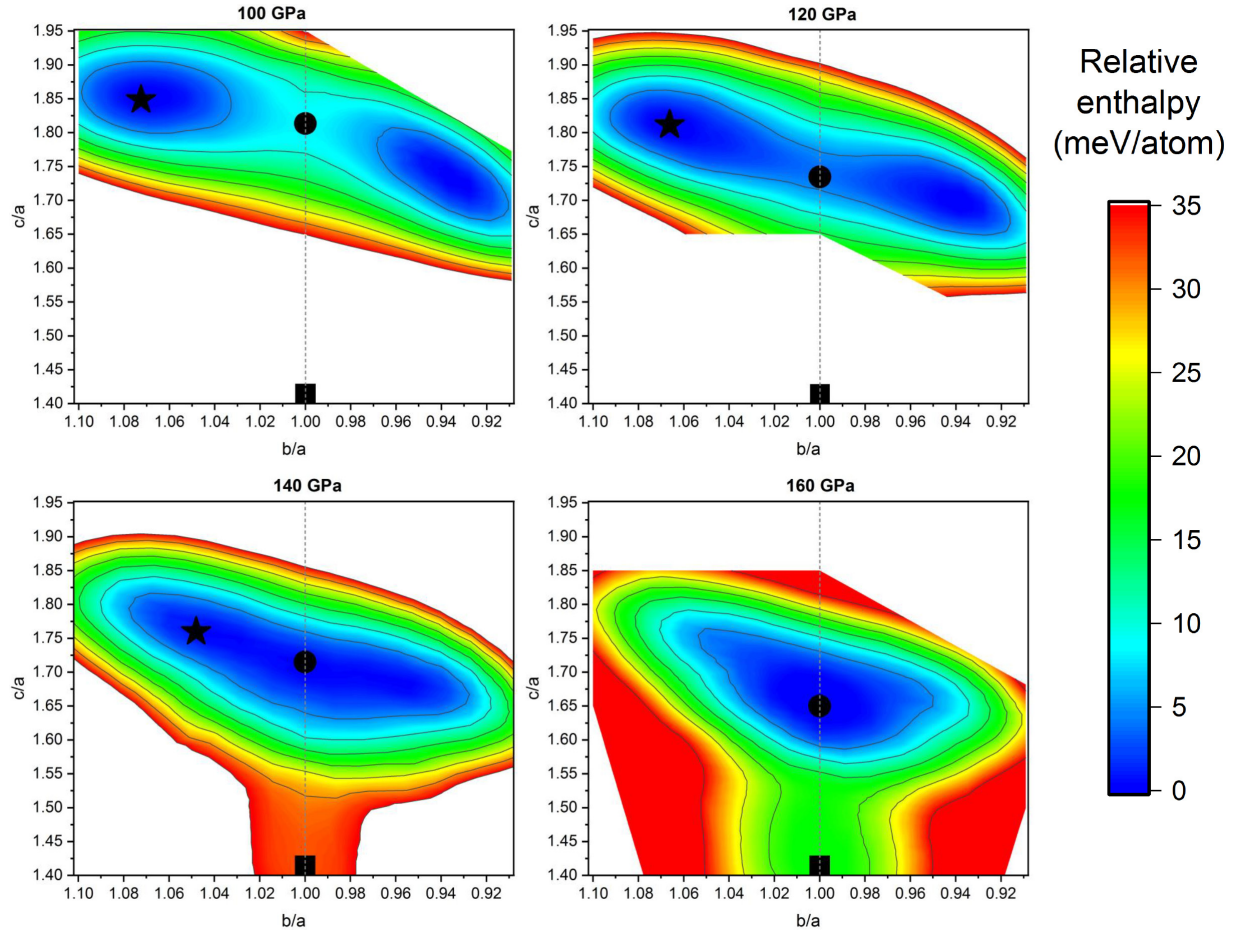


FIG. 3. Calculated relative enthalpy values (meV/atom) of bromine under pressure as a function of  $c/a$  and  $b/a$  ratio. Black stars, circles, and squares indicate the relative enthalpy of the  $Immm$ ,  $I4/mmm$ , and  $Fm\bar{3}m$  structures, respectively.  $b/a$  ratios are mirrored around  $b/a = 1$  by symmetry.

excitation of a significant temperature-induced distribution of lattice shapes with a finite population occupying the  $I4/mmm$  structure. The volume discontinuity and anomalously sluggish  $Immm$ - $I4/mmm$  transition in experiments is thus attributed to entropic effects. While *ab initio* calculations predict that the  $I4/mmm$  structure becomes the ground state of close-packed bromine between 140 and 150 GPa (Supplemental Fig. S2), the experimental onset and termination of the  $Immm$ - $I4/mmm$  transition occurs between 105 and 167 GPa, respectively. As shown in Fig. 3, our calculations reveal the development of a deeper, more narrow potential energy well around the  $I4/mmm$  structure at high pressure, which coincides with the experimental termination of the  $Immm$ - $I4/mmm$  transition. These strong entropic effects may also explain the Raman activity of dissociated iodine [19], as the high intrinsic degree of structural disorder will relax Raman selection rules of the dissociated phases.

Now we turn our attention to the transition to the  $Fm\bar{3}m$  structure, possibly the final condensed phase of bromine. The  $Fm\bar{3}m$  phase is predicted to become the ground state structure around 195 GPa [26], and our calculations in Fig. 4 show that the enthalpy difference of the two phases becomes less than 20 meV/atom at pressures above 160 GPa.

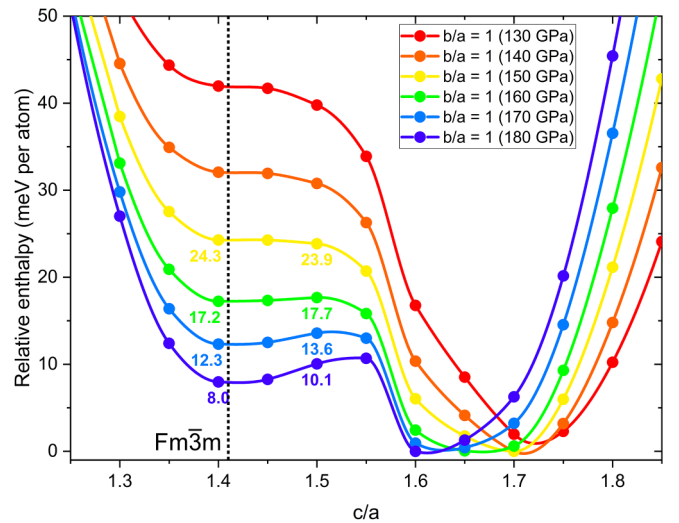


FIG. 4. Relative enthalpy per atom of dissociated bromine as a function of  $c/a$  ratio and pressure when  $b/a = 1$ .  $c/a = \sqrt{2}$  is the  $Fm\bar{3}m$  structure, while all other  $c/a$  ratios correspond to  $I4/mmm$  structures. A metastable enthalpy minimum for the fcc phase starts to develop between 160 and 170 GPa.

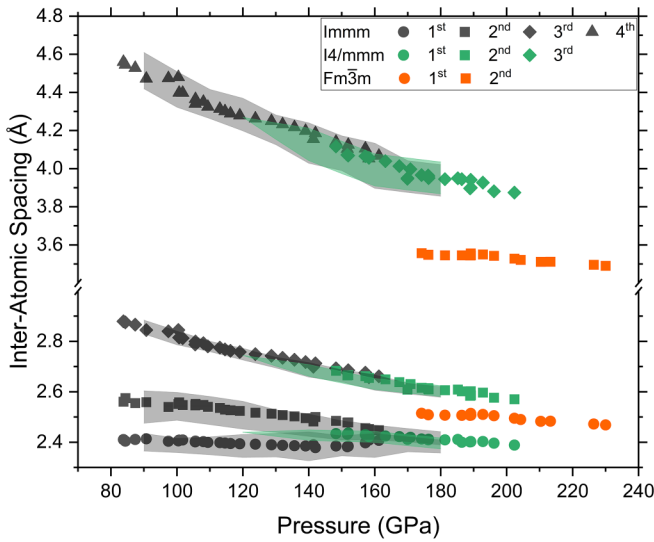


FIG. 5. Nearest-neighbor distances vs pressure for dissociated bromine from experiments and density functional theory (DFT) calculations. Points indicate experimentally derived values. Colored bands indicate the range of values determined for structures within 5 meV/atom of the minimum enthalpy structure.

Consequently the experimental onset of the transition, around 172–180 GPa, similarly coincides with the pressure range where the two structures become energetically competitive in *ab initio* calculations. In these calculations, by 180 GPa the enthalpy difference between the  $Fm\bar{3}m$  and  $I4/mmm$  structures is 8 meV/atom. While recent work has reported the synthesis of iodine with the  $Pm\bar{3}n$  structure at high temperatures at conditions near the  $I4/mmm$ - $Fm\bar{3}m$  boundary in iodine [29], this structure is not observed experimentally in the present study. In Fig. S3, we present static enthalpy calculations for the  $Pm\bar{3}n$  structure in bromine compared to other structures of dissociated bromine. We find this structure to be metastable relative to the close-packed phases observed in the present study, although the enthalpy difference reaches a minimum in the vicinity of the  $I4/mmm$ - $Fm\bar{3}m$  boundary which is qualitatively similar to its synthesis conditions for iodine. We propose that  $Pm\bar{3}n$  iodine is likely a quenched high-temperature phase, and that the synthesis of this phase in bromine would similarly require high temperatures.

The structural evolution of the close-packed phases can also be visualized through the evolution of nearest-neighbor atoms under pressure. In Fig. 5, the first, second, and fourth nearest neighbors for the  $Immm$  phase correspond to the  $b$ ,  $a$ , and  $c$  lattice constants, respectively, while third nearest neighbors are positioned at a distance equal to  $c^* = 1/2(a^2 + b^2 + c^2)^{1/2}$  [13]. As  $b = a$  in the  $I4/mmm$  phase, first and third nearest neighbors correspond to the  $a$  and  $c$  axes, with second nearest neighbors given by  $c^* = 1/2(2a^2 + c^2)^{1/2}$ .

Despite the occurrence of the  $I4/mmm$ - $Fm\bar{3}m$  phase transition in the Mbar pressure range for bromine, the percent modification of interatomic distances is larger than for iodine. Bromine exhibits a volume change of about 0.8% across the transition, however the interatomic spacings corresponding to the  $a$  axis expand by 5.6% while the  $c$  axis contracts by 9.4% (Fig. 5) in the transformation to the  $Fm\bar{3}m$  structure. In

contrast, for iodine the same transition results in an expansion of the  $a$  axis by 3.0%, while the  $c$  axis contracts by 2.4%, with an overall volume contraction of 1.8%; the free-energy change  $P\Delta V$  across the  $I4/mmm$ - $Fm\bar{3}m$  transition in bromine is 40% lower than the same transition in iodine [13]. The decrease in  $P\Delta V$  up the period highlights the importance of the electronic polarizability of the halogens; as the lighter halogens have fewer core electrons, the effect of lone pair repulsion is stronger and leads to a preference for more anisotropic structures [12].

In conclusion, we present here a combined experimental and computational study on the phase evolution of bromine beyond its molecular and incommensurately modulated phases. We report a series of transitions between atomic phases, culminating in the synthesis of a close-packed, electronically isotropic metal. The phase transition sequence mirrors that of iodine but at much higher pressures. The diffraction data of the  $Immm$  to  $I4/mmm$  phase transition are best explained by a coexistence regime of two structures that have a crystallographic group-subgroup relationship, suggesting an unexpected first-order phase transition. Our calculations show, however, that the PES of bromine around this transition is strongly anharmonic, so that a wide range of lattice shapes, compatible with both  $Immm$  and  $I4/mmm$  symmetry, are thermodynamically accessible. A second transition from  $I4/mmm$  to  $Fm\bar{3}m$  also shows coexistence, but reflects a genuine first-order transition to cubic close packed bromine. The lighter halogens, fluorine and hydrogen, adopt intrinsically anharmonic structures owing to their low atomic mass and high zero-point energy which results in atomic motion even at 0 K. In this aspect, they are fundamentally different from the heavier halogens which are perceived as essentially static atoms at 0 K. The present study shows that for experimental investigations of the heavier halogens, even at room temperature, entropic effects have a significant influence on the phase transition characteristics of the dissociated phases due to the small enthalpy differences associated with successive transitions between the close-packed structures. This behavior is expected to be present for all halogens, but is most prominent in bromine as close-packed phases are formed at much higher pressures in chlorine and fluorine, and occur over a very narrow pressure range in iodine. We propose that more insights into the structural scaling of the halogens can be found through investigations of the heavy halogens at simultaneous high pressures and temperatures.

## ACKNOWLEDGMENTS

Portions of this work were performed at GeoSoilEnviroCARS (The University of Chicago, Sector 13), Advanced Photon Source (APS), Argonne National Laboratory. GeoSoilEnviroCARS was supported by the National Science Foundation – Earth Sciences (EAR – 1634415). This research used resources of the Advanced Photon Source, a U.S. Department of Energy (DOE) Office of Science User Facility operated for the DOE Office of Science by Argonne National Laboratory under Contract No. DE-AC02-06CH11357. Use of the GSECARS Raman Lab System was supported by the NSF MRI Proposal (EAR-1531583). We acknowledge the ESRF for providing synchrotron radiation and technical

support at beamline ID15b. We acknowledge Polish high-performance computing infrastructure PLGrid for awarding this project access to the LUMI supercomputer, owned by the EuroHPC Joint Undertaking, hosted by CSC (Finland) and the LUMI consortium through PLL/2022/03/016434. This research was funded by National Science Centre (NCN), Poland, within the SONATA BIS programme (Grant No. UMO-2019/34/E/ST4/00445). This research was carried out with the support of the Poznan Supercomputing and Networking Center (PSNC) as part of allocation pl0091-02. We are grateful for computational support from the U.K. national high performance computing service, ARCHER2, for

which access was obtained via the UKCP consortium and funded by EPSRC Grant Ref. No. EP/X035891/1. M.P.A. acknowledges funding from the ERC project HECATE and from UKRI Future leaders fellowship MRC-MR/T043733/1. R.T.H. thanks the European Research Council (ERC) under the European Union's Horizon 2020 research and innovation programme (Grant agreement No. 948895, MetElOne).

## DATA AVAILABILITY

The data supporting this study's findings are available in the Supplemental Material [42].

- [1] E. Wigner and H. B. Huntington, On the possibility of a metallic modification of hydrogen, *J. Chem. Phys.* **3**, 764 (1935).
- [2] K. Takemura, S. Minomura, O. Shimomura, and Y. Fujii, Observation of molecular dissociation of iodine at high pressure by x-ray diffraction, *Phys. Rev. Lett.* **45**, 1881 (1980).
- [3] R. Reichlin, K. E. Brister, A. K. McMahan, M. Ross, S. Martin, Y. K. Vohra, and A. L. Ruoff, Evidence for the insulator-metal transition in xenon from optical, x-ray, and band-structure studies to 170 GPa, *Phys. Rev. Lett.* **62**, 669 (1989).
- [4] H. Luo, S. Desgreniers, Y. K. Vohra, and A. L. Ruoff, High-pressure optical studies on sulfur to 121 GPa: Optical evidence for metallization, *Phys. Rev. Lett.* **67**, 2998 (1991).
- [5] S. Serra, G. Chiarotti, S. Scandolo, and E. Tosatti, Pressure-induced magnetic collapse and metallization of molecular oxygen: The  $\zeta$ -O<sub>2</sub> phase, *Phys. Rev. Lett.* **80**, 5160 (1998).
- [6] H. Fujihisa, Y. Fujii, K. Takemura, and O. Shimomura, Structural aspects of dense solid halogens under high pressure studied by x-ray diffraction—molecular dissociation and metallization, *J. Phys. Chem. Solids* **56**, 1439 (1995).
- [7] T. Kume, T. Hiraoka, Y. Ohya, S. Sasaki, and H. Shimizu, High pressure Raman study of bromine and iodine: Soft phonon in the incommensurate phase, *Phys. Rev. Lett.* **94**, 065506 (2005).
- [8] P. Dalladay-Simpson, J. Binns, M. Peña-Alvarez, M.-E. Donnelly, E. Greenberg, V. Prakapenka, X.-J. Chen, E. Gregoryanz, and R. T. Howie, Band gap closure, incommensurability and molecular dissociation of dense chlorine, *Nat. Commun.* **10**, 1134 (2019).
- [9] L. Crapanzano, W. A. Crichton, G. Monaco, R. Bellissent, and M. Mezouar, Alternating sequence of ring and chain structures in sulphur at high pressure and temperature, *Nat. Mater.* **4**, 550 (2005).
- [10] D. Laniel, B. Winkler, T. Fedotenko, A. Pakhomova, S. Chariton, V. Milman, V. Prakapenka, L. Dubrovinsky, and N. Dubrovinskaia, High-pressure polymeric nitrogen allotrope with the black phosphorus structure, *Phys. Rev. Lett.* **124**, 216001 (2020).
- [11] C. Ji, B. Li, W. Liu, J. S. Smith, A. Majumdar, W. Luo, R. Ahuja, J. Shu, J. Wang, S. Sinogeikin, Y. Meng, V. B. Prakapenka, E. Greenberg, R. Xu, X. Huang, W. Yang, G. Shen, W. L. Mao, and H.-K. Mao, Ultrahigh-pressure isostructural electronic transitions in hydrogen, *Nature (London)* **573**, 558 (2019).
- [12] D. Duan, Z. Liu, Z. Lin, H. Song, H. Xie, T. Cui, C. J. Pickard, and M. Miao, Multistep dissociation of fluorine molecules under extreme compression, *Phys. Rev. Lett.* **126**, 225704 (2021).
- [13] Y. Fujii, K. Hase, N. Hamaya, Y. Ohishi, A. Onodera, O. Shimomura, and K. Takemura, Pressure-induced face-centered-cubic phase of monatomic metallic iodine, *Phys. Rev. Lett.* **58**, 796 (1987).
- [14] Y. Fujii, K. Hase, Y. Ohishi, H. Fujihisa, N. Hamaya, K. Takemura, O. Shimomura, T. Kikegawa, Y. Amemiya, and T. Matsushita, Evidence for molecular dissociation in bromine near 80 GPa, *Phys. Rev. Lett.* **63**, 536 (1989).
- [15] R. Reichlin, A. K. McMahan, M. Ross, S. Martin, J. Hu, R. J. Hemley, H.-K. Mao, and Y. Wu, Optical, x-ray, and band-structure studies of iodine at pressures of several megabars, *Phys. Rev. B* **49**, 3725 (1994).
- [16] R. Ibberson, O. Moze, and C. Petrillo, High resolution neutron powder diffraction studies of the low temperature crystal structure of molecular iodine (I<sub>2</sub>), *Mol. Phys.* **76**, 395 (1992).
- [17] B. Powell, K. Heal, and B. Torrie, The temperature dependence of the crystal structures of the solid halogens, bromine and chlorine, *Mol. Phys.* **53**, 929 (1984).
- [18] Q. Zeng, Z. He, X. San, Y. Ma, F. Tian, T. Cui, B. Liu, G. Zou, and H.-k. Mao, A new phase of solid iodine with different molecular covalent bonds, *Proc. Natl. Acad. Sci. USA* **105**, 4999 (2008).
- [19] E. Bykova, I. G. Batyrev, M. Bykov, E. Edmund, S. Chariton, V. B. Prakapenka, and A. F. Goncharov, Structural evolution of iodine on approach to the monatomic state, *Phys. Rev. B* **108**, 024104 (2023).
- [20] A. San-Miguel, H. Libotte, M. Gauthier, G. Aquilanti, S. Pascarelli, and J.-P. Gaspard, New phase transition of solid bromine under high pressure, *Phys. Rev. Lett.* **99**, 015501 (2007).
- [21] J. Shi, E. Fonda, S. Botti, M. A. Marques, T. Shinmei, T. Irifune, A.-M. Flank, P. Lagarde, A. Polian, J.-P. Itié *et al.*, Halogen molecular modifications at high pressure: the case of iodine, *Phys. Chem. Chem. Phys.* **23**, 3321 (2021).
- [22] K. Takemura, K. Sato, H. Fujihisa, and M. Onoda, Modulated structure of solid iodine during its molecular dissociation under high pressure, *Nature (London)* **423**, 971 (2003).
- [23] H. Fujihisa, K. Takemura, M. Onoda, and Y. Gotoh, Two intermediate incommensurate phases in the molecular dissociation process of solid iodine under high pressure, *Phys. Rev. Res.* **3**, 033174 (2021).

- [24] Y. Yin, A. Aslandukov, M. Bykov, D. Laniel, A. Aslandukova, A. Pakhomova, T. Fedotenko, W. Zhou, F. I. Akbar, M. Hanfland, K. Glazyrin, C. Giacobbe, E. L. Bright, G. Garbarino, Z. Jia, N. Dubrovinskaia, and L. Dubrovinsky, Polytypism of incommensurately modulated structures of crystalline bromine upon molecular dissociation under high pressure, *Phys. Rev. B* **110**, 104111 (2024).
- [25] T. Ishikawa, K. Mukai, Y. Tanaka, M. Sakata, Y. Nakamoto, T. Matsuoka, K. Shimizu, and Y. Ohishi, Metallization of solid iodine in phase I: X-ray diffraction measurements, electrical resistance measurements, and *ab initio* calculations, *High Press. Res.* **33**, 186 (2013).
- [26] M. H. Dalsaniya, K. J. Kurzydłowski, and D. Kurzydłowski, Insights into the high-pressure behavior of solid bromine from hybrid density functional theory calculations, *Phys. Rev. B* **106**, 115128 (2022).
- [27] Y. Fujii, K. Hase, Y. Ohishi, N. Hamaya, and A. Onodera, Pressure-induced monatomic tetragonal phase of metallic iodine, *Solid State Commun.* **59**, 85 (1986).
- [28] P. Li, G. Gao, and Y. Ma, Modulated structure and molecular dissociation of solid chlorine at high pressures, *J. Chem. Phys.* **137**, 064502 (2012).
- [29] A. F. Goncharov, H. Chen, I. G. Batyrev, M. Bykov, L. Brüning, E. Bykova, V. Kovalev, M. F. Mahmood, M. Mezouar, G. Garbarino, and J. Wright, Polymorphism of monatomic iodine, *Phys. Rev. B* **111**, 014103 (2025).
- [30] S. Anzellini, A. Dewaele, F. Occelli, P. Loubeyre, and M. Mezouar, Equation of state of rhenium and application for ultra high pressure calibration, *J. Appl. Phys.* **115**, 043511 (2014).
- [31] C. Prescher and V. B. Prakapenka, Dioptas: a program for reduction of two-dimensional x-ray diffraction data and data exploration, *High Press. Res.* **35**, 223 (2015).
- [32] P. Václav, D. Michal, and P. Lukáš, Crystallographic computing system JANA2006: General features, *Z. Kristallogr. - Cryst. Mater.* **229**, 345 (2014).
- [33] Y. Akahama and H. Kawamura, Pressure calibration of diamond anvil Raman gauge to 310 GPa, *J. Appl. Phys.* **100**, 043516 (2006).
- [34] A. V. Krukau, O. A. Vydrov, A. F. Izmaylov, and G. E. Scuseria, Influence of the exchange screening parameter on the performance of screened hybrid functionals, *J. Chem. Phys.* **125**, 224106 (2006).
- [35] S. Grimme, J. Antony, S. Ehrlich, and H. Krieg, A consistent and accurate *ab initio* parametrization of density functional dispersion correction (DFT-D) for the 94 elements H-Pu, *J. Chem. Phys.* **132**, 154104 (2010).
- [36] J. Moellmann and S. Grimme, DFT-D3 study of some molecular crystals, *J. Phys. Chem. C* **118**, 7615 (2014).
- [37] G. Kresse and J. Furthmüller, Efficient iterative schemes for *ab initio* total-energy calculations using a plane-wave basis set, *Phys. Rev. B* **54**, 11169 (1996).
- [38] G. Kresse and D. Joubert, From ultrasoft pseudopotentials to the projector augmented-wave method, *Phys. Rev. B* **59**, 1758 (1999).
- [39] H. J. Monkhorst and J. D. Pack, Special points for Brillouin-zone integrations, *Phys. Rev. B* **13**, 5188 (1976).
- [40] J. George, C. Reimann, V. L. Deringer, T. Bredow, and R. Dronskowski, On the DFT ground state of crystalline bromine and iodine, *ChemPhysChem* **16**, 728 (2015).
- [41] A. Hermann, R. Hoffmann, and N. W. Ashcroft, Condensed astatine: Monatomic and metallic, *Phys. Rev. Lett.* **111**, 116404 (2013).
- [42] See Supplemental Material at <http://link.aps.org/supplemental/10.1103/rbsx-vqhf> for Figs. S1– S4, as well as Supplemental Datasets S1 and S2.
- [43] K. Takemura, S. Minomura, O. Shimomura, Y. Fujii, and J. D. Axe, Structural aspects of solid iodine associated with metallization and molecular dissociation under high pressure, *Phys. Rev. B* **26**, 998 (1982).